

Influence of architecture for nanostructured Pr_6O_{11} and GDC composite oxygen electrodes on their electrochemical properties and stability

Michael Spann^{1,2}, Lydia Yefsah^{1,2}, Rakesh Sharma¹, César Steil¹, Laurent Dessemond¹,
Jérôme Laurencin², Elisabeth Djurado¹

¹ Univ. Grenoble Alpes, Univ. Savoie Mont Blanc, CNRS, Grenoble INP, LEPMI, 38000 Grenoble, France

² Univ. Grenoble Alpes, CEA, LITEN, DTCH, 17 rue des Martyrs, 38054 Grenoble, France

michael.spann@grenoble-inp.fr



Programme et Equipements Prioritaires de Recherche
sur l'Hydrogène Décarbonaté (PEPR-H2)
Oxygen electrode materials

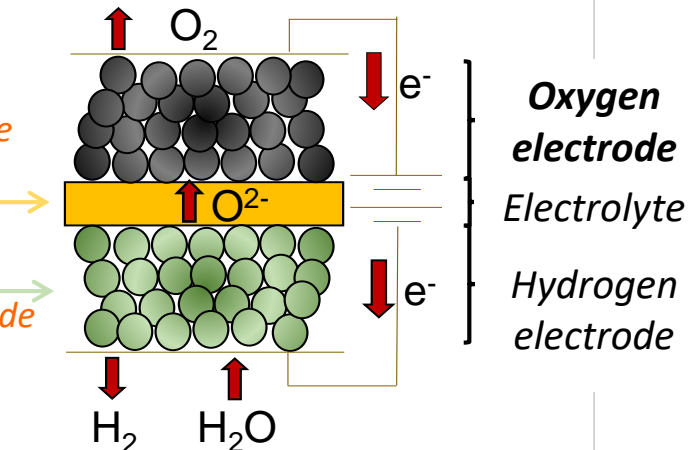


Working principle of solid oxide cells (SOC)

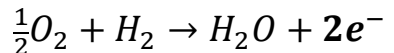
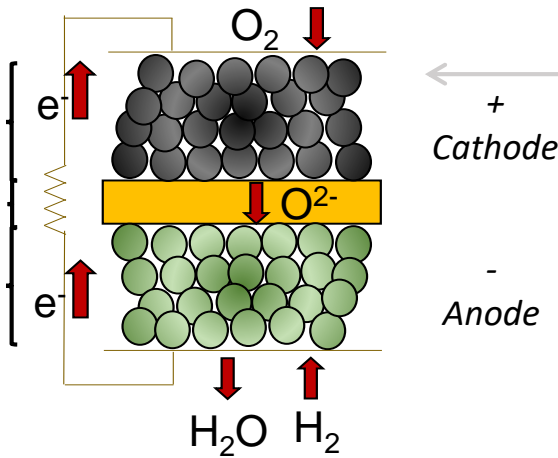
Electrolysis cell: SOEC

- $\sigma_{O^{2-}}$: dense, large grains
➤ YSZ, GDC

- Porosity
- Percolation $\sigma_{O^{2-}} + \sigma_{e^-}$
- Chem. stability (S, C)
- YSZ/ GDC + 30 % Ni



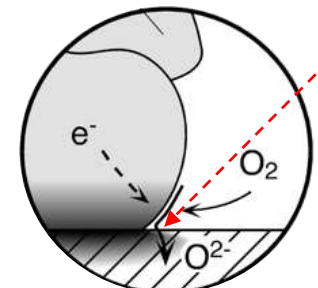
Fuel cell: SOFC



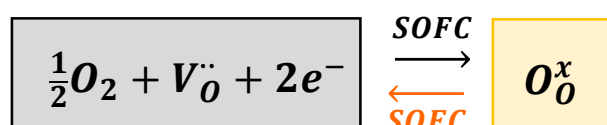
O₂ electrode characteristics

- Electrocatalytic activity
- Porosity
- σ_{e^-} (+ $\sigma_{O^{2-}}$)
- Chem. stability
- Mechanical stability

Triple-phase boundary (TPB)



S.B. Adler, Chem. Rev., 104 (2004) 4791

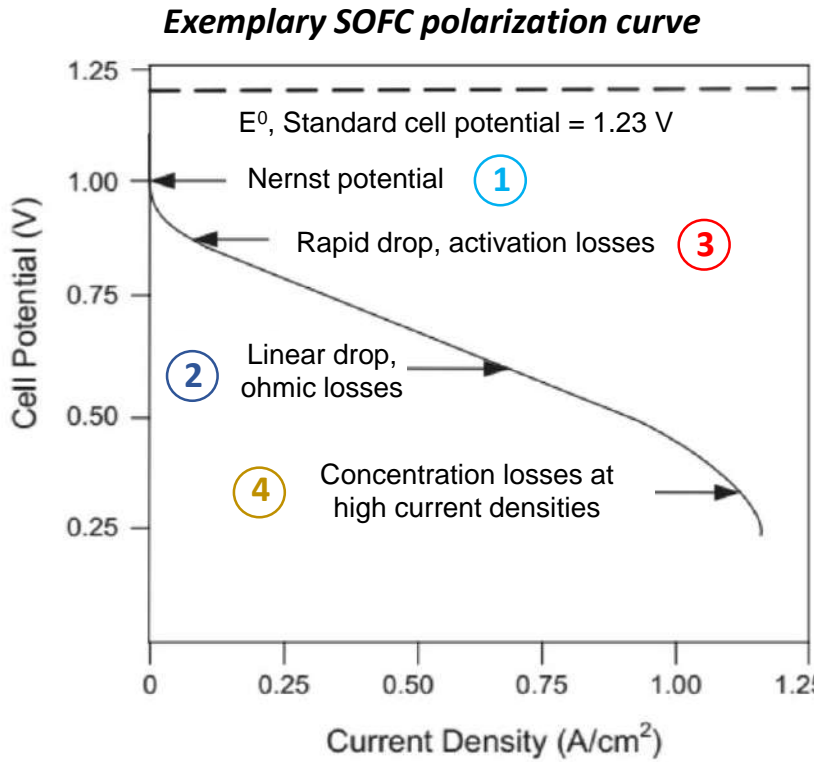


SOFC: oxygen reduction reaction (ORR)
SOEC: oxygen evolution reaction (OER)

- Oxygen electrode materials:**
1. Electronic conductors
 2. Mixed ionic + electronic conductors (MIEC)
 3. Composites

Operation condition:
 $650^\circ\text{C} < T < 1000^\circ\text{C}$

One bottleneck of SOC – oxygen electrode



EIS: decreasing ω

$$U_{SOFC}(j) = U_N - \eta_{ohm}(j) - \sum \eta_{activation\ polariz.} - \sum \eta_{concentration\ polariz.}$$

(1) $U_N = E^0 - \frac{RT}{4F} \ln \frac{pH_2O}{pO_2^{1/2} pH_2}$

(2) $\eta_{ohm} = i \times (R_{electrolyte} + R_{contact}) \rightarrow \sigma_{ion} \propto \exp\left(-\frac{Q}{k_B T}\right)$

(3) Processes in active layer: reaction kinetics + activation energies

(4) Availability of oxygen species (depletion, accumulation)

Thermal activation

Model for area-specific polarization resistance
(porous, single-phase MIEC)

$$ASR_{pol} \propto \left(\sqrt{\frac{\tau}{(1-\varepsilon)a D_o k_o c_o^2}} \right)$$

S.B. Adler, J. Electrochim. Soc., 143 (1996) 3554-3564

Microstructure

τ : Tortuosity
 ε : Porosity
 a : Specific surface area (m^{-1})

Oxygen transport

D_o : Oxygen self-diffusion coeff. (m^2/s)
 k_o : Oxygen self-surface exchange coeff. (m/s)

Thermodynamics

c_o : concentration of oxygen lattice sites in equilibrium (mol/m^3)

- T-related inconveniences**
- ❖ Elevated startup times
 - ❖ Continuous energy demand
 - ❖ Degradation promoted

Lower operation T?

- ❖ Reduced reaction kinetics
- ❖ Increased activation energy

- ✓ Electrolyte ohmic losses : doping + thin dimensions
- **Oxygen electrode overpotentials :**
 1. **Choice of electrode materials (intrinsic properties)**
 2. **Modification of microstructure/ architecture**

Alternative oxygen electrode materials

Research towards stable, performant SOC materials

$La_{1-x}Sr_xMnO_3$ (ABO_3)

- $\sigma_{e^-} = 200 \text{ S cm}^{-1}$, 800 °C
Y Takeda, Int. J. Electrochem. Soc., 134 (1987), 2656

$La_{1-x}Sr_xCo_{1-y}Fe_yO_{3-\delta}$ (ABO_3)

- $\sigma_{e-, 6428} = 300 \text{ S cm}^{-1}$, 650°C
L.W. Tai, Solid State Ion., 76 (1995), 273
- $\sigma_{\text{ion}, 6428} = 0.007 \text{ S cm}^{-1}$, 650°C
B. Fan, Solid State Sci., 13 (2011), 1835

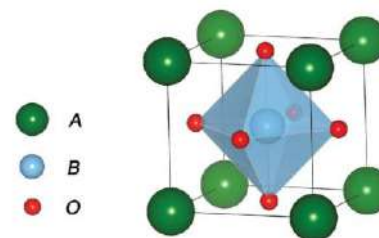
$Ln_2NiO_{4+\delta}$ ($A_{n+1}B_nO_{3n+1}$)

- La/Pr: stability/ electrocatalytic prop.
- $\sigma_{e^-} = 40-110 \text{ S cm}^{-1}$, 700 °C
E. Boehm, Solid State Ion., 176 (2005), 2717
- Decomposition under current
($Pr_4Ni_3O_{10-\delta}$, $Pr_3O_{7-\delta}$, Pr_6O_{11})
V. Vibhu, J. Energy Chem., 46 (2020), 62-70
N.I. Khamidy, J. Power Sources, 450 (2020), 227724

Pr_6O_{11} (AO_2)

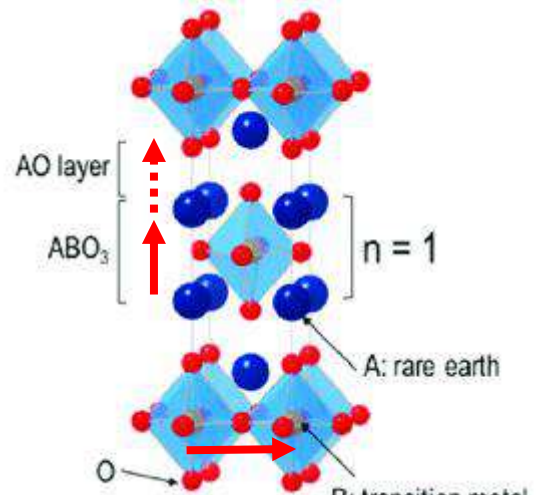
- Transition of Pr_2O_3 to PrO_2
- PrO_x with $x = 1.833$ ($PrO_{2-\delta}$)
→ mixed valency Pr^{3+}/Pr^{4+}
- $\sigma_{e^-} < 4 \text{ S/cm}$
C Nicollet, Int. J. Hydrog. Energy, 41 (2016), 15538

Cubic Perovskite



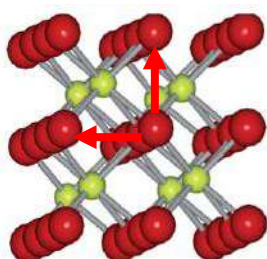
- Doping of La^{3+} with Sr^{2+} : oxygen vacancies
- Transition metals: mixed valency, σ_{e^-}

Ruddlesden-Popper ($n=1$)



- Vacancy mechanism in c-direction
- Insterstitials in ab-plane → T-activated

Cubic Fluorite



Isotropic transport properties

Material

Material	D^* (cm^2/s)	k^* (cm/s)
LSM ¹	5.0×10^{-8}	1.0×10^{-12}
LSCF ²	7.0×10^{-7}	5.0×10^{-8}
LNO ³	1.0×10^{-6}	1.5×10^{-8}
PNO ⁴	5.0×10^{-7}	2.5×10^{-8}
Pr_6O_{11} ⁵	3.4×10^{-8}	5.4×10^{-7}

900 °C

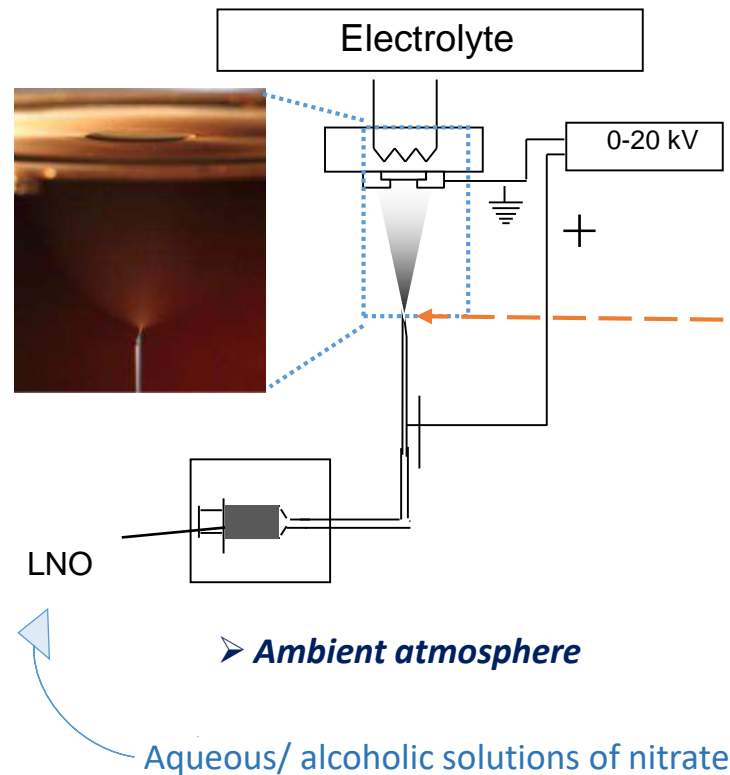
600 °C

¹ De Souza, Solid State Ion., 106 (1998), 175; ² Audinot, (1999) PhD Thesis, Université de Bordeaux; ³ Skinner, Solid State Ion., 135 (2000), 709; ⁴ Boehm, Solid State Ion., 176 (2005), 2717; ⁵ Nicollet, Int. J. Hydrog. Energy, 41 (2016), 15538

Traditionally SOC via screen-printing, tape casting, ...

➤ What is the effect of reduced grain/ particle sizes?

Electrostatic Spray Deposition (ESD)



Gañan-Calvo (initial droplet size)

$$d_{size} \propto \left(\frac{\rho \varepsilon_0 Q^3}{\gamma \sigma} \right)^{1/6}$$

- Surface tension, γ (N/m)
- Electrical conductivity, σ (S/m)
- Solution density, ρ (g/cm³)
- Solution flow rate, Q (ml/h)

Gañan-Calvo, J. Aerosol Sci., 28 (1997), 249

e.g. $\phi_{EtOH, 1.5 mL/h}: 3.8 \mu m$

➤ Microstructures with different textures, porosities, particle size

Factors on droplet size

- 1) Initial droplet size - physicochemical properties of precursor solutions:
 - Solvent $\rightarrow T_B, \gamma$
 - Concentration $\rightarrow \sigma, \gamma$
 - Amount of solution $\rightarrow Q$
- 2) Final droplet size - deposition parameters:
 - Conditions during flight $\rightarrow T, d, t$
 - Amount of solution $\rightarrow Q$

➤ Complex interplay of factors

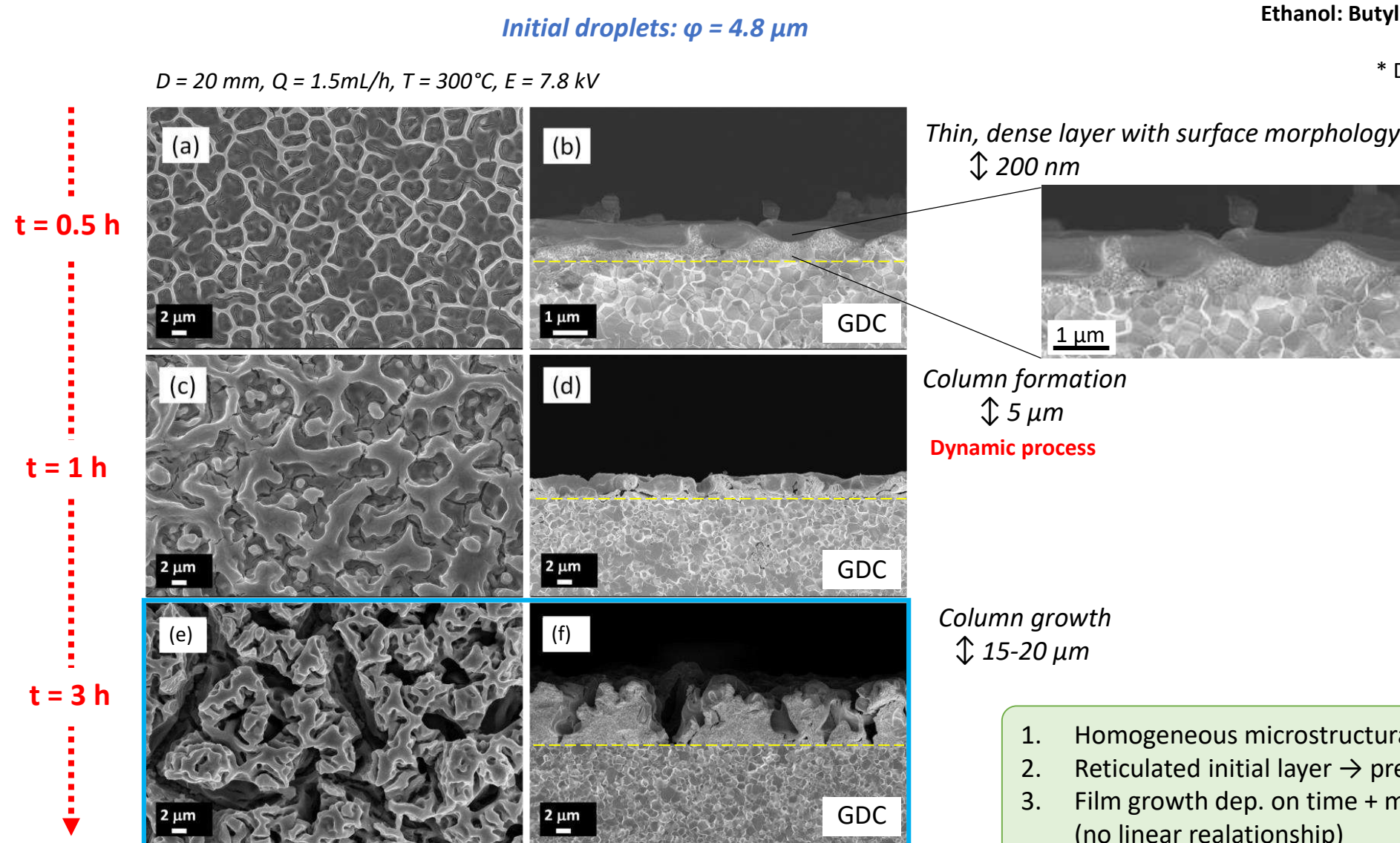
Preparation of ESD deposits on GDC

1. Deposition time
2. Deposition temperature
3. Nozzle-to-substrate distance
4. Solution flow rate

Analysis of morphology

1. SEM (surface, cross-sections)
2. TEM, XRD (grain size)

Effect of deposition time

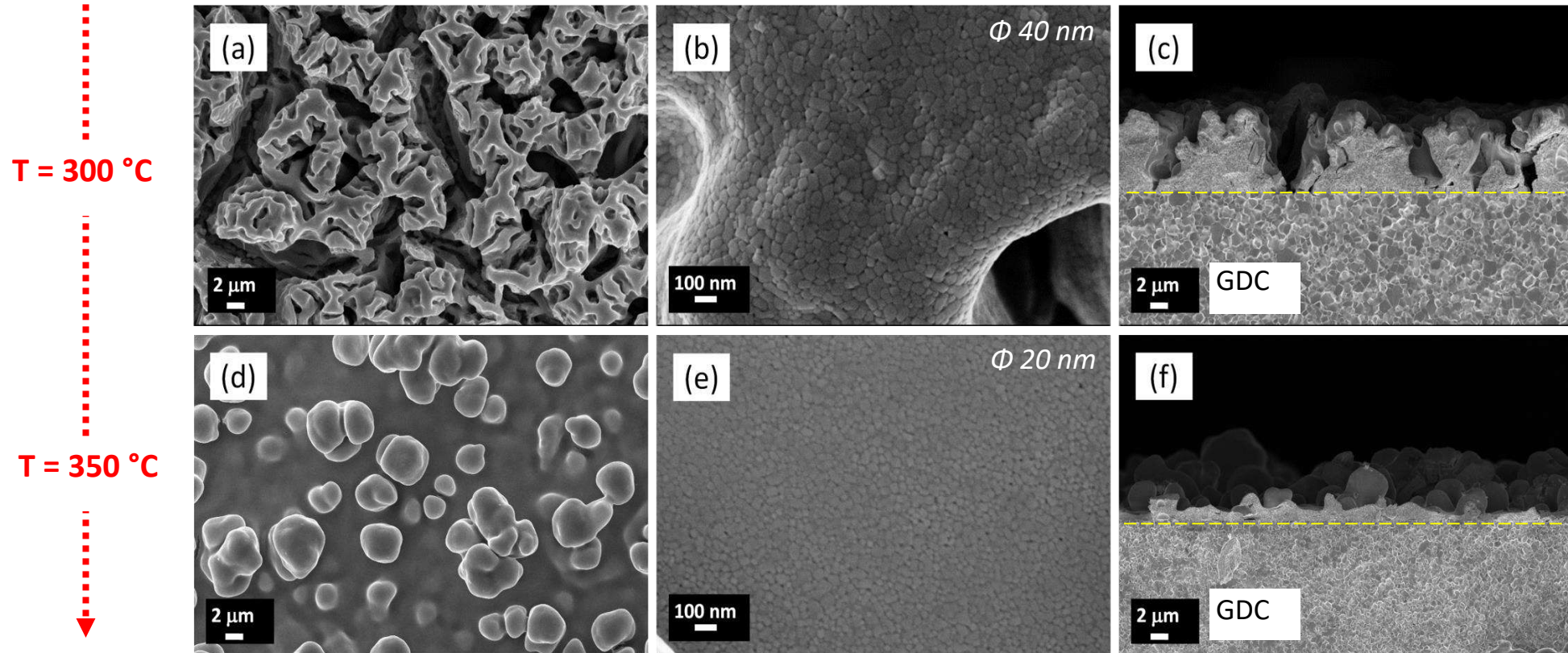


1. Homogeneous microstructural evolution over time
2. Reticulated initial layer → preferential deposition
3. Film growth dep. on time + microstructure
(no linear relationship)

Effect of deposition temperature

Initial droplets: $\varphi = 4.8 \mu\text{m}$

$D = 20 \text{ mm}$, $Q = 1.5 \text{ mL/h}$, $E = 7.8\text{-}10 \text{ kV}$, $t = 3 \text{ h}$



Ethanol: Butyl carbitol * (1:2, wt.), 0.02 M

Calcinated for 2 h, 700°C

* Diethylene glycol butyl ether

Columns

Simultaneous spreading
and drying of droplets

Dynamic process

Dense layer with
agglomerates

Ordered process

1. Particle size \downarrow for $T \uparrow$
2. Grain size: $40 \text{ nm} \rightarrow 20 \text{ nm}$
3. Microstructural evolution: agglomerated particles for higher T

Effect of nozzle-to-substrate distance

$Q = 1.5 \text{ mL/h}$, $T = 300^\circ\text{C}$, $E = 7.8 \text{ kV}$, $t = 3 \text{ h}$

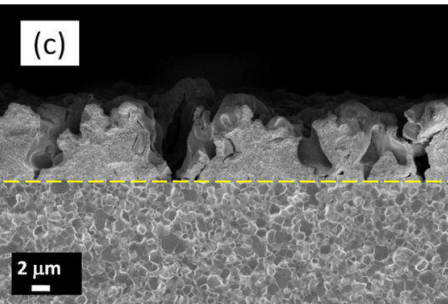
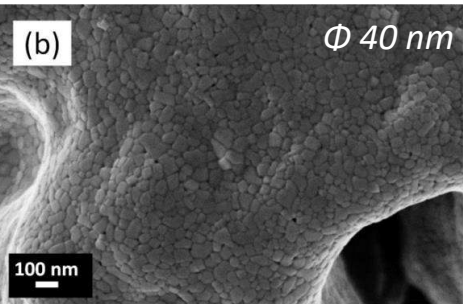
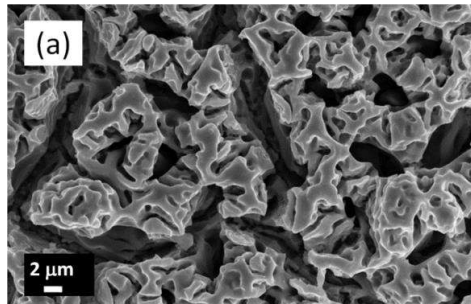
Initial droplets: $\varphi = 4.8 \mu\text{m}$

Ethanol: Butyl carbitol * (1:2, wt.), 0.02 M

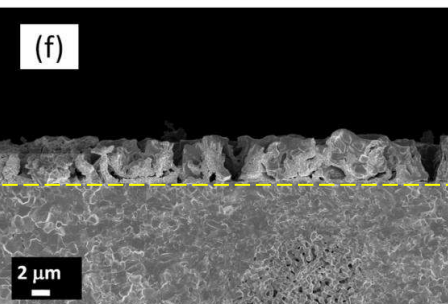
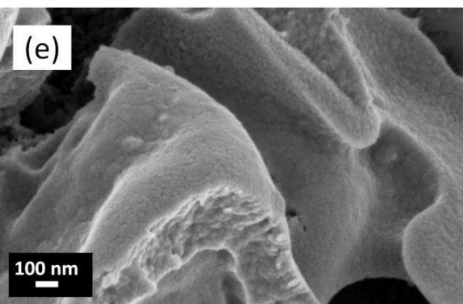
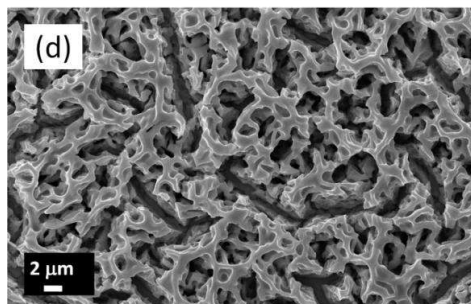
Calcinated for 2 h, 700°C

* Diethylene glycol butyl ether

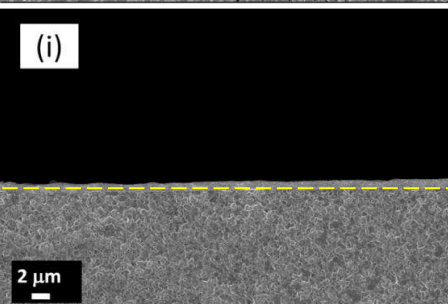
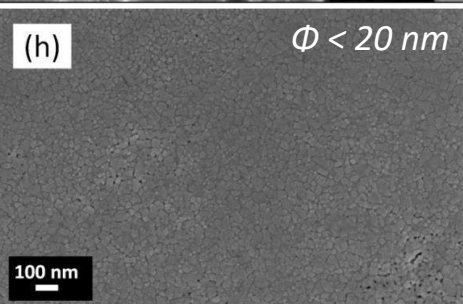
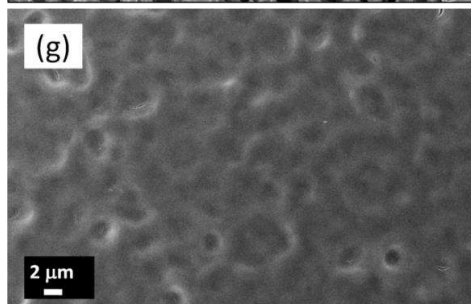
D = 2 cm



D = 3 cm



D = 5 cm



1. Homogeneous evolution of microstructure
2. Particle size \downarrow for D \uparrow
3. Grain size: $40 \text{ nm} \rightarrow < 20 \text{ nm}$

Wide columns,
large particles

Dynamic process

Thin columns,
smaller particles
 \rightarrow reticulation

Dense layer,
small particles
(no agglomeration yet)

Ordered process

Effect of solution flow rate

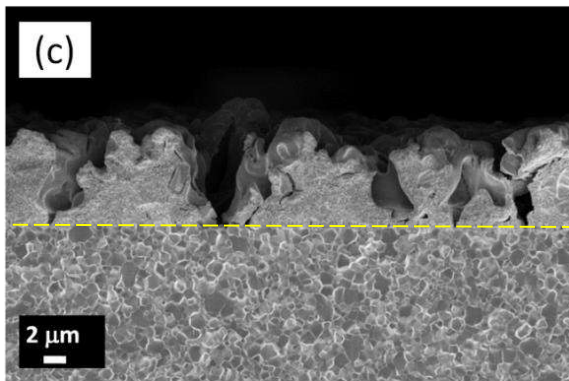
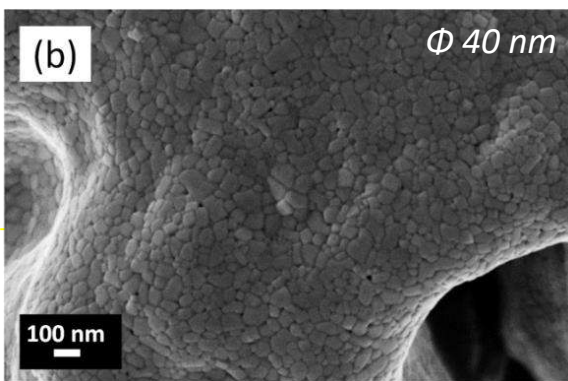
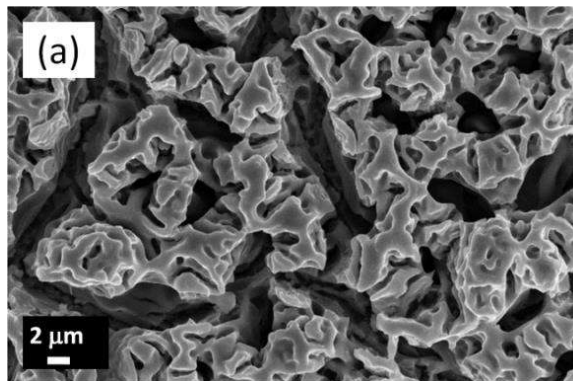
Ethanol: Butyl carbitol * (1:2, wt.), 0.02 M
Calcinated for 2 h, 700 °C
* Diethylene glycol butyl ether

$$d_{size} \propto \left(\frac{\rho \varepsilon_0 Q^3}{\gamma \sigma} \right)^{1/6}$$

Gañan-Calvo, J. Aerosol Sci., 28 (1997), 249

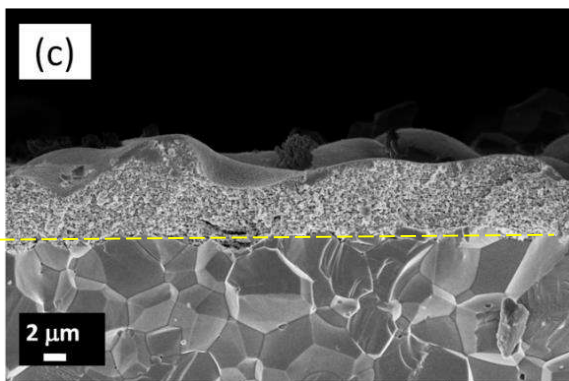
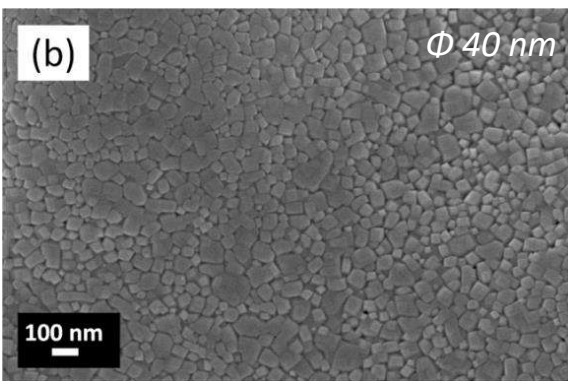
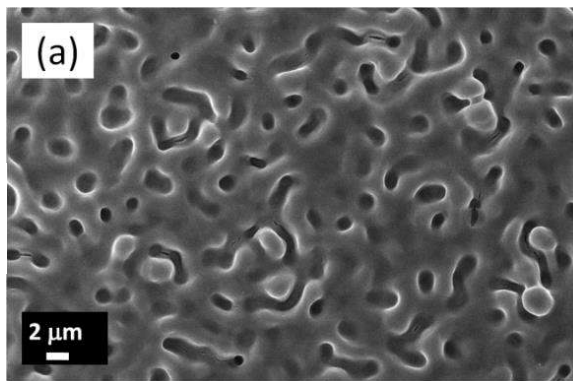
$D = 20 \text{ mm}$, $T = 300 \text{ }^\circ\text{C}$, $E = 7.8 \text{ kV}$, $t = 3 \text{ h}$

Q = 1.5 mL/h
Initial droplets
 $\varphi = 4.8 \mu\text{m}$



Column growth
Dynamic process

Q = 0.5 mL/h
Initial droplets
 $\varphi = 2.8 \mu\text{m}$

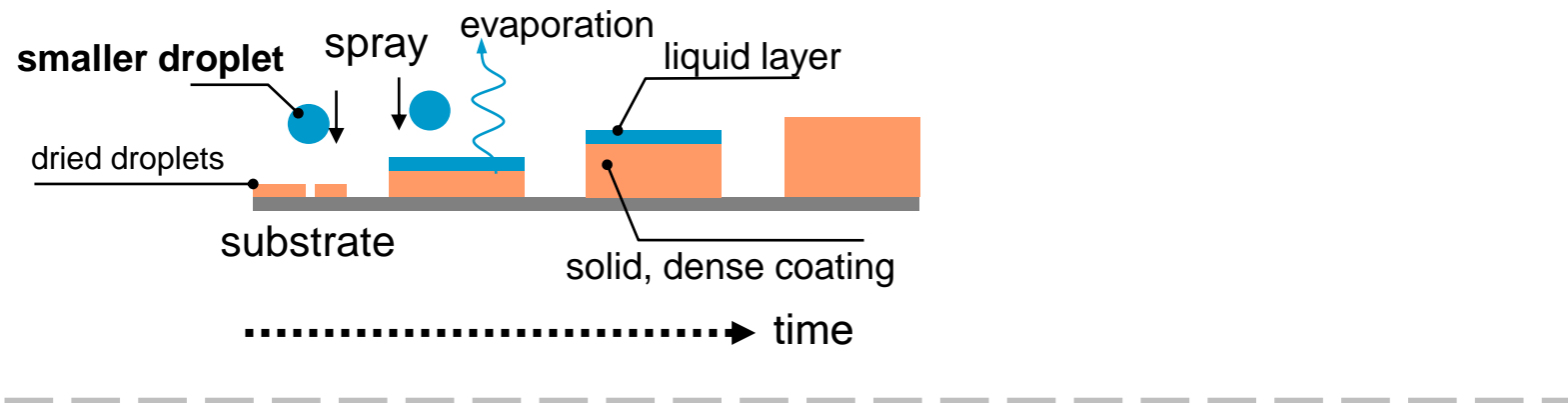


Dense layer
Ordered process

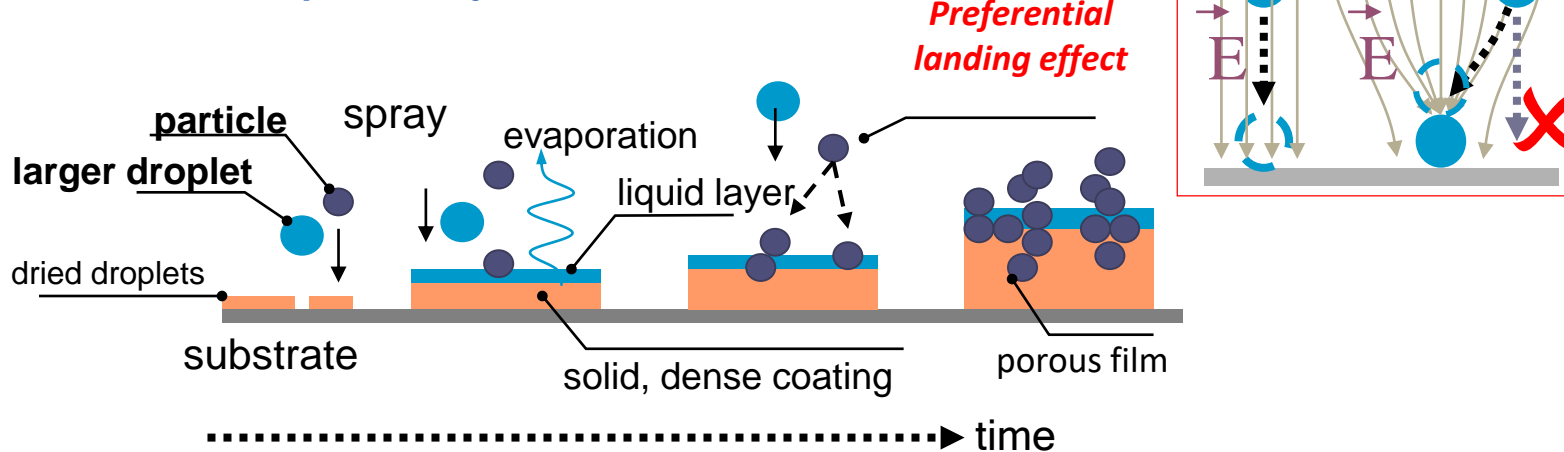
- 1. Particle size \downarrow for flow rate \downarrow
- 2. Grain size similar for different initial droplet sizes
- 3. Evolution of microstructure to dense layer

Summary - Influence of ESD parameters

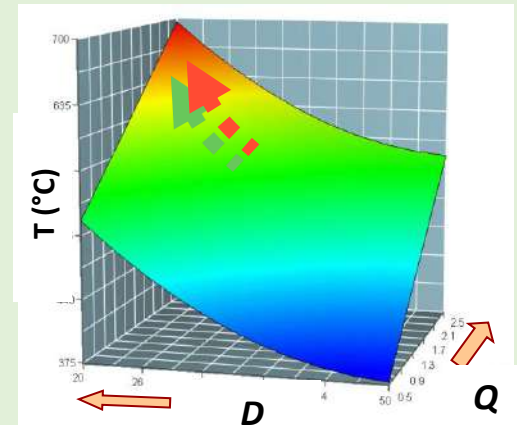
1. Growth of a dense layer



2. Growth of a porous layer



1. Equilibrium of parameters



R. Neagu, Solid State Ionics, 177 (2006), 1981-1984

Plane = constant droplet size

- High T allows high Q and high D
- Small T limits D and Q

2. Short deposition time:

Dense, thin initial layer

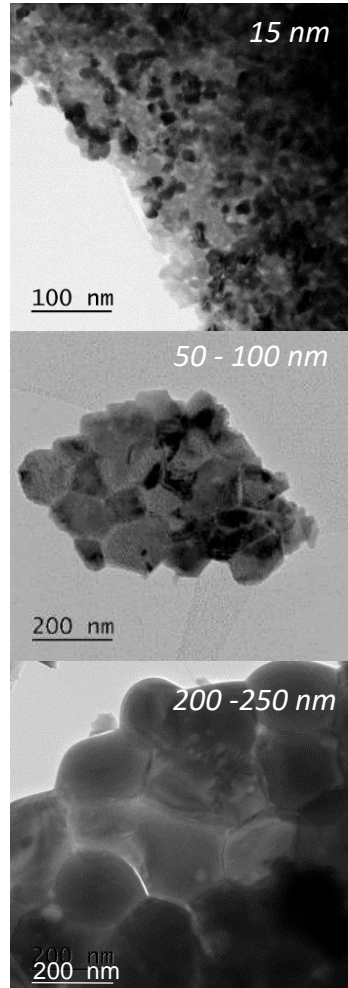
3. Longer deposition times:

Development of microstructures

✓ **High influence on morphology and porosity via deposition parameters**

Influence of calcination temperature on crystallite size

Particles post-calcination

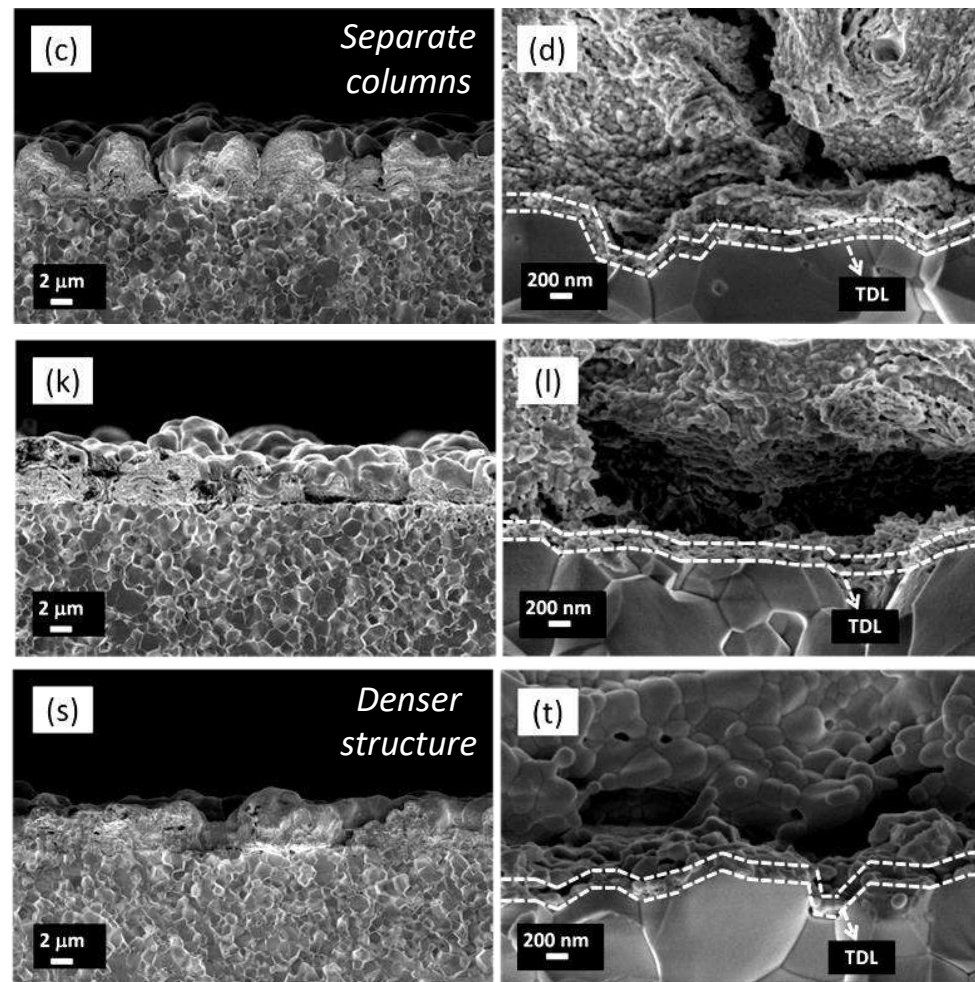


$T = 600\text{ }^{\circ}\text{C}$

$T = 800\text{ }^{\circ}\text{C}$

$T = 1000\text{ }^{\circ}\text{C}$

Calcination of ESD deposits



$V_{\text{acceleration}} = 200\text{ kV}, 0.19\text{ mm resolution}$

Aggregate formation (XRD: 27-65 nm)

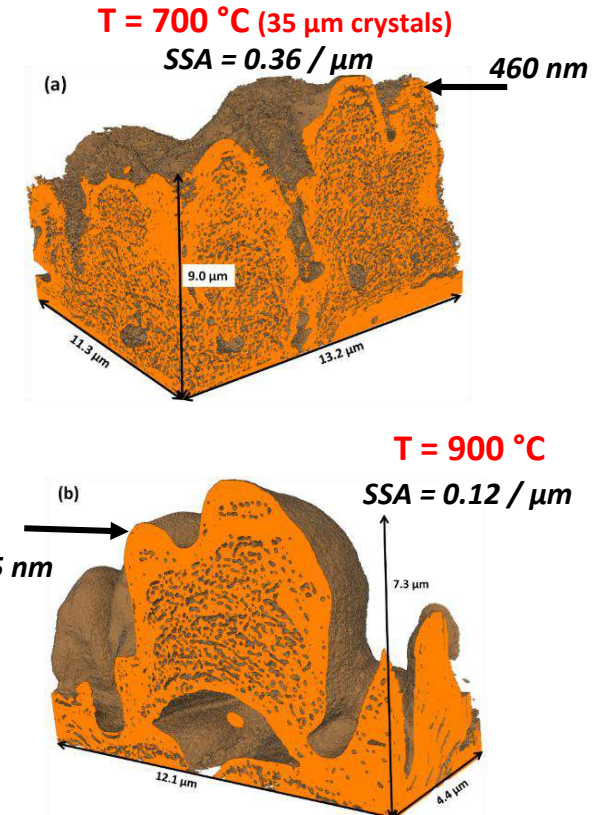
26/05/2023

Influence of architecture for nanostructured Pr_6O_{11} and GDC composite oxygen electrodes

- Apparent densification (morphology maintained)
- Dense interlayer already at low $T \rightarrow \text{CT}_{\text{ion}}$

$\text{H}_2\text{O: Butyl carbitol * (1:2, wt.), 0.02\text{ M}$
 $Q = 1\text{ mL/h}, T = 300\text{ }^{\circ}\text{C}, d = 20\text{ mm}$
Calcinated for 2 h

FIB-SEM + 3D-reconstruction



- “Core-shell” structure
- Ideally low sintering temperature
- Stability?

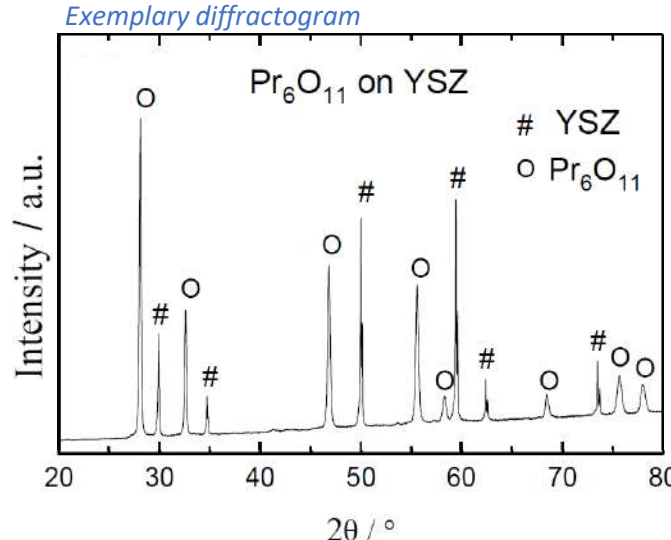
Stability of Pr_6O_{11} with GDC and YSZ

Sample preparation

1. Pr_6O_{11} (ESD, columnar, $> 10 \mu\text{m}$, 35 nm particles)
2. Composite pellets (50 % wt.): Pr_6O_{11} and GDC/YSZ



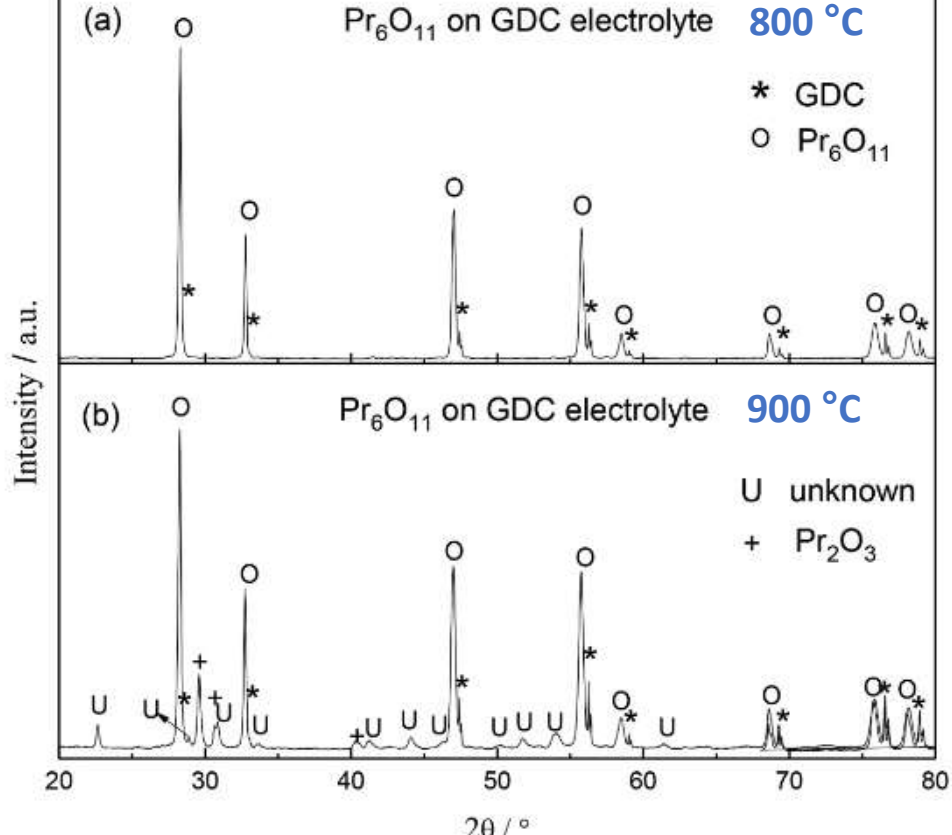
3. Thermal treatment (800 °C or 900 °C, 10 days)



✓ Chemical stability for all samples and temperatures

Pr_6O_{11} (ESD) – GDC

Philips X'Pert-MPD system, Cu K α radiation, $\lambda=1.54056 \text{ \AA}$



✓ 800 °C, 10 days: no decomposition

❖ 900 °C, 10 days: partial decomposition, unidentified phases (ongoing)

L. Yefsah, Solid State Ionics (submitted)

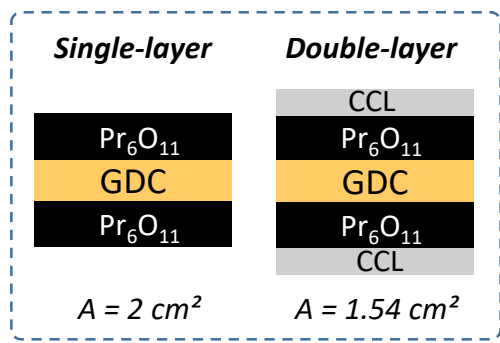
*Study of symmetrical cell architectures
(Focus on interface AFL/CCL)*

1. Focus on AFL/CCL interface
(CCL composition, CCL thickness)
2. Optimization of AFL sintering temperature
3. Comparison of ESD morphology in practical application

Analysis of electrochemical behavior

1. EIS
($V_a = 0.02$ V, 1 MHz - 50 mHz, Au grids 1024 mesh/cm²)
2. R_{pol} extraction

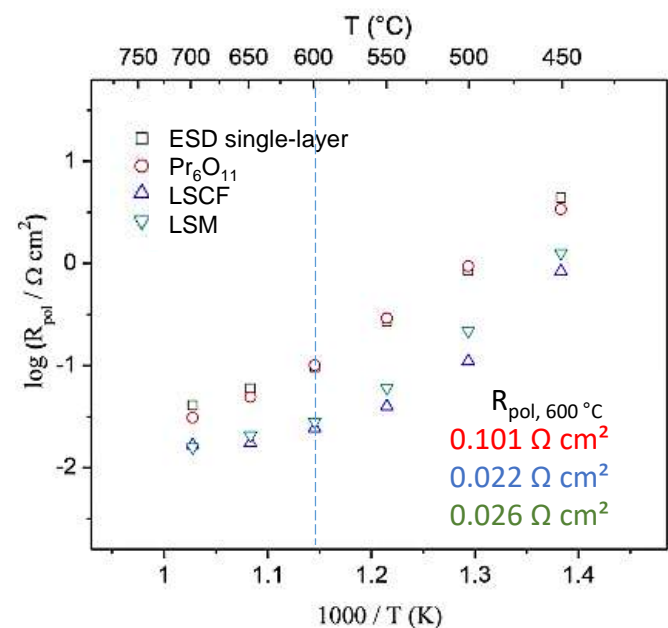
Focus on current collector layer (CCL)



CCL composition

ESD calcination: 700 °C, 2h
 CCL thickness = 30 µm
Architecture (AFL + CCL)

- Pr₆O₁₁ (ESD) + Pr₆O₁₁(SP)
- Pr₆O₁₁ (ESD) + LSCF (SP)
- Pr₆O₁₁ (ESD) + LSM (SP)

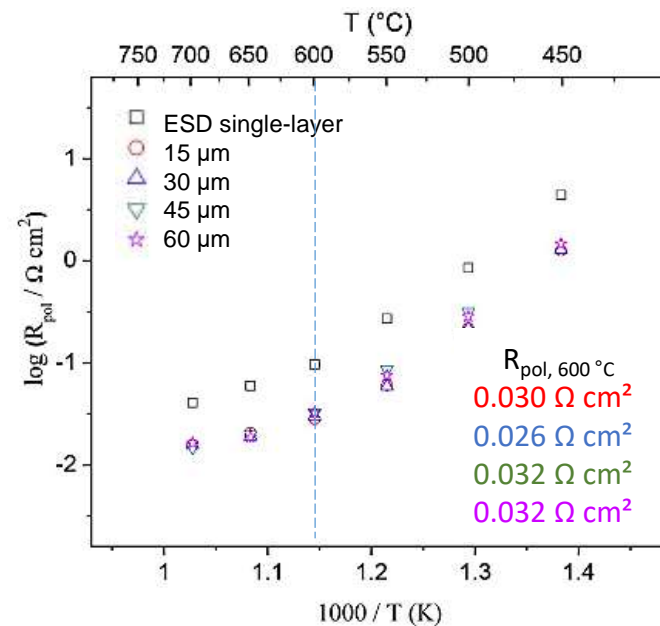


➤ T > 600 °C: LSM and LSCF as best choice

CCL thickness

ESD calcination: 700 °C, 2h

Architecture (AFL + CCL)	CCL thickness (µm)
Pr ₆ O ₁₁ (ESD) + LSM (SP)	15
Pr ₆ O ₁₁ (ESD) + LSM (SP)	30
Pr ₆ O ₁₁ (ESD) + LSM (SP)	45
Pr ₆ O ₁₁ (ESD) + LSM (SP)	60

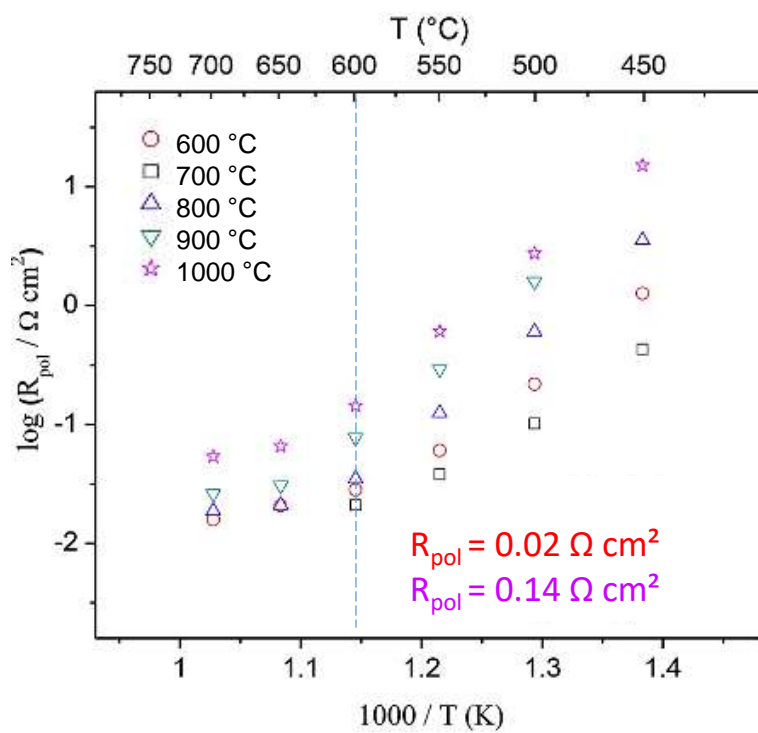


➤ Minimum CCL thickness (avoid current constriction) ca. 30 µm

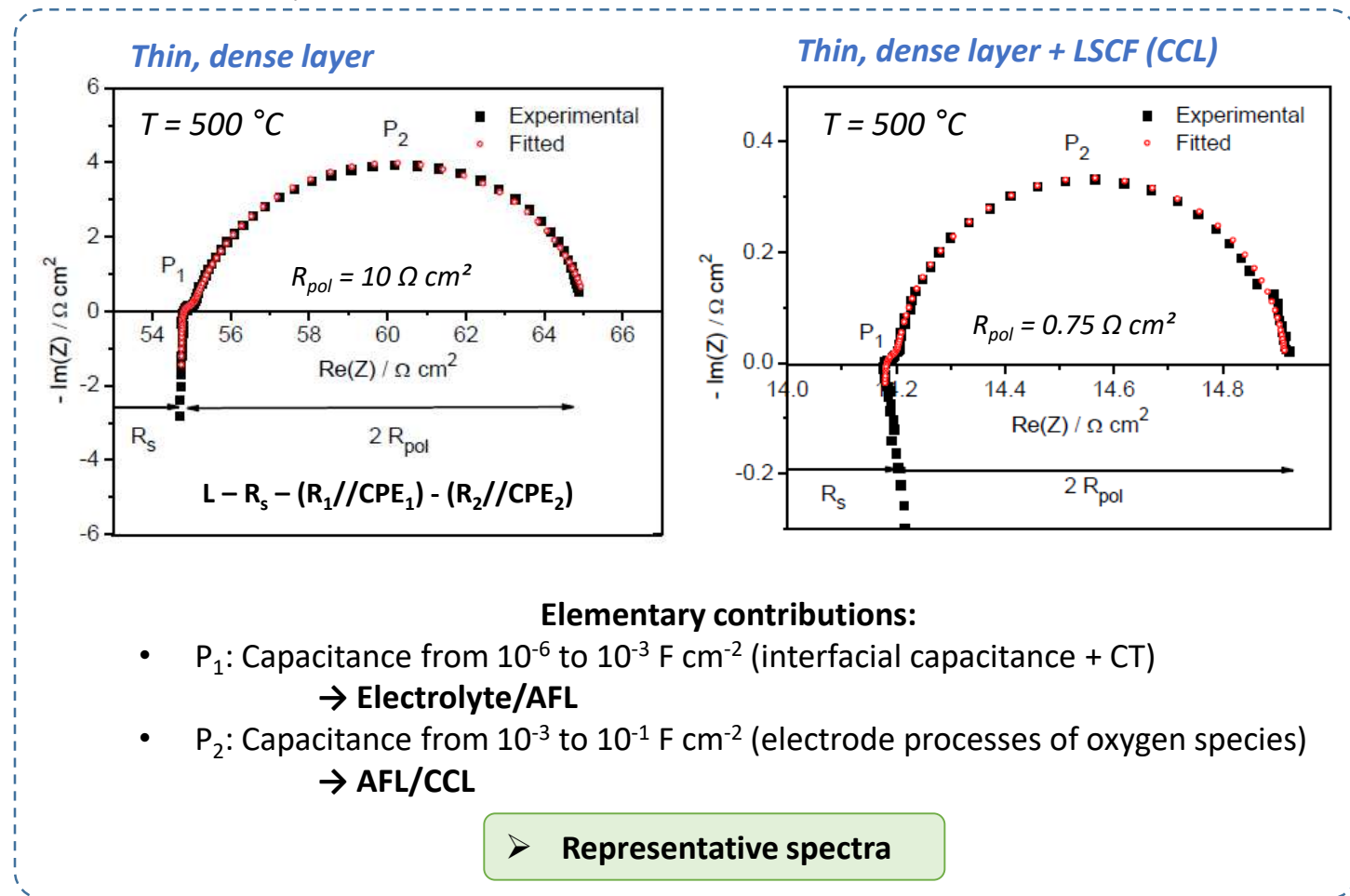
Optimization of AFL sintering temperature

LSM thickness = 30 μm

Post-ESD sintering, air	AFL particles, SEM (nm)
600 °C, 2h	< 20
700 °C, 2h	35
800 °C, 2h	50-100
900 °C, 2h	100-150
1000 °C, 2h	200-250

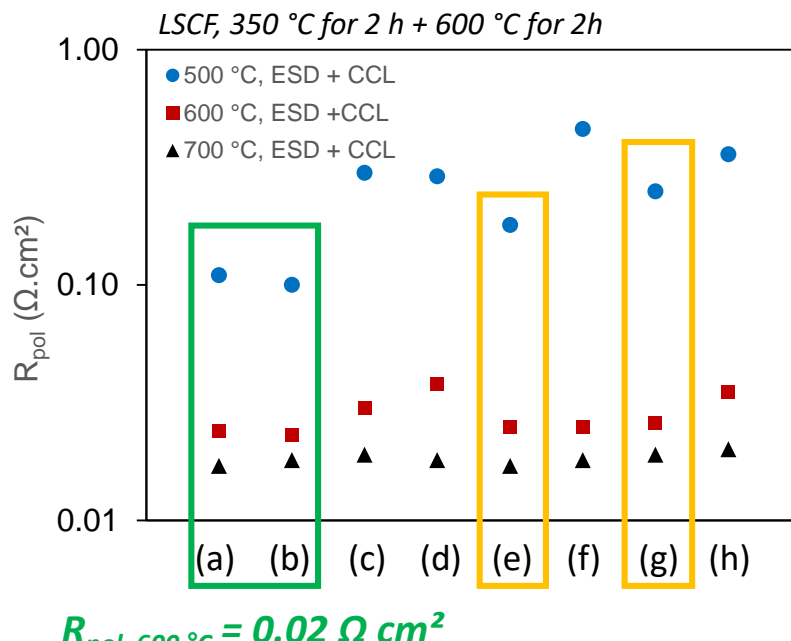


PGSTAT 302N, $V_a = 0.02 \text{ V}$, 1 MHz - 50 mHz, Au grids 1024 mesh/cm²



➤ Ideal ESD calcination temperature < 800 °C (small grains, highest surface area)

Influence of electrode microstructure on R_{pol}



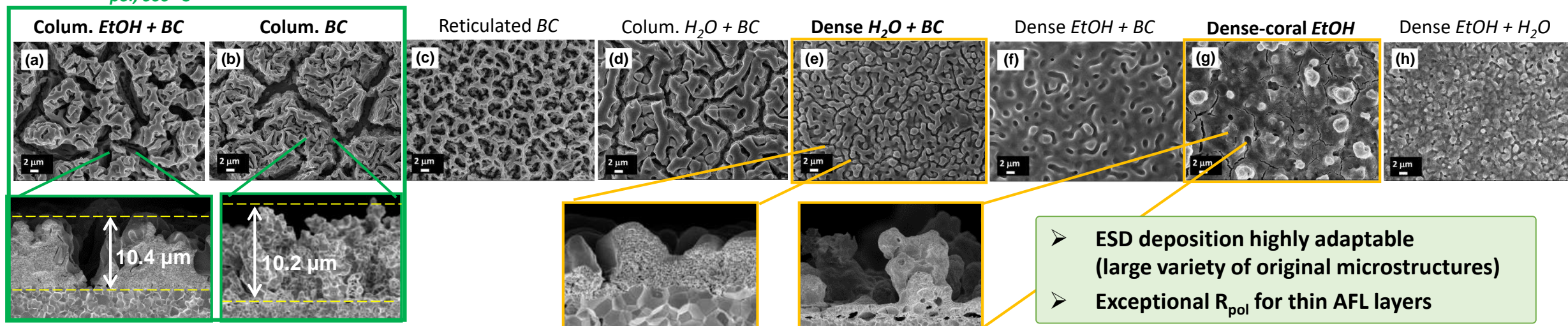
$$R_{pol, 600 \text{ } ^\circ\text{C}} = 0.02 \text{ } \Omega \text{ cm}^2$$

$$d_{size} \propto \left(\frac{\rho \varepsilon_0 Q^3}{\gamma \sigma} \right)^{1/6}$$

Gañan-Calvo, J. Aerosol Sci., 28 (1997), 249

Solution	σ (mS/cm)	T_b^* (°C)	Droplet size (μm)	Particle size [†] (nm)
EtOH	76.5	88.0	3.8	20
EtOH:H ₂ O (1:2)	1.61x10 ³	111.2	2.0	20
H ₂ O:BC (1:2)	3.5x10 ²	192.8	2.7	35
EtOH:BC (1:2)	17.3	193.3	4.8	35
BC	1.89	206.4	6.9	35

* TGA + DTA; [†] SEM + Image J analysis

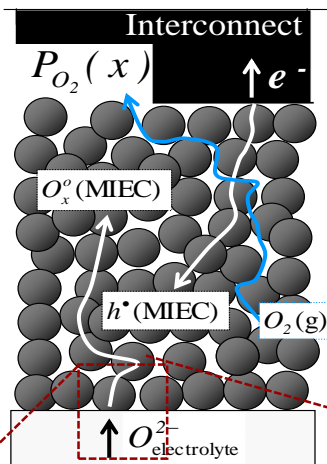


- Search of alternative SOC oxygen electrode materials (reduce operation temperature)
- Investigation of Pr_6O_{11} → Decomposition product of $\text{La}_{1-x}\text{Pr}_x\text{NiO}_{4+\delta}$



1. Synthesis of nanostructured Pr_6O_{11} electrodes for SOC by ESD → Electrostatic Spray Deposition
2. High control of process via deposition parameters (T, d, Q, t, solvent) → Microstructural studies
3. Evaluation of thermal stability window on GDC and YSZ electrolytes → 800 °C, IT-SOC
4. Preparation of symmetrical SO cells on GDC electrolytes → ESD + Screen-printing
5. Architecture of symmetrical cells optimized via EIS → ESD – calcination at 600 °C, 2h
LSM-CCL of 30 µm thickness (700 °C, 2h)
 $R_{pol, 600\text{ }^{\circ}\text{C}} = 0.02 \Omega \text{ cm}^2$ for columnar microstructure

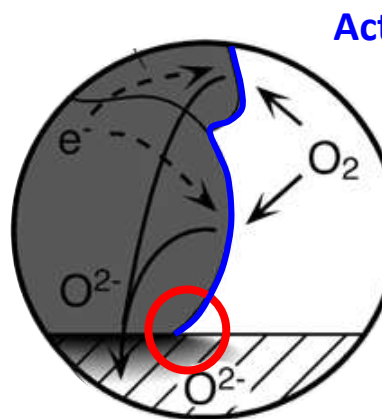
SOEC mode (for LNO)



- R1: Direct oxidation at TPB
- R2: Ionic transfer (electrolyte to electrode)
- R3: Interstitial diffusion + excorporation + formation of adatoms
- R4: Association + desorption

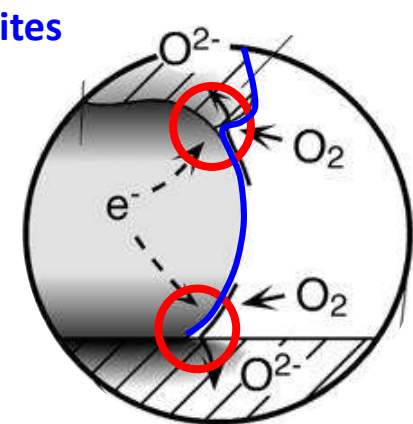
G Sdanghi, J. Electrochem. Soc., 169 (2022), 034518
L Yefsah, (2023) PhD Thesis, UGA

MIEC/ σ_{ion}



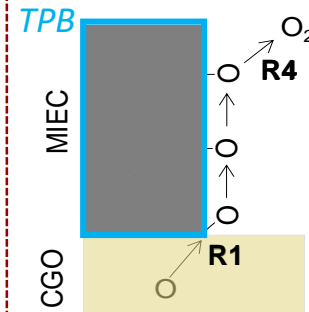
Active sites
TPB

MIEC + $\sigma_{\text{ion}} / \sigma_{\text{ion}}$

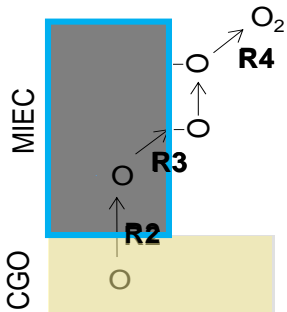


S.B. Adler, Chem. Rev., 104 (2004) 4791

Surface path

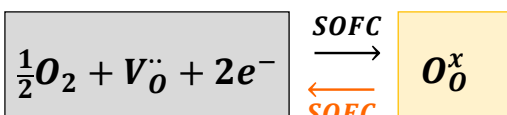


Bulk path



Dominant surface path
→ increase number of TPB

Increase interface
MIEC/ ionic conductor



- ✓ SOEC: interstitial filling, parallel surface + bulk path, stable
- ✗ SOFC: depletion of interstitials (bulk path limiting)
 1. Performance
 2. Physical delamination (e.g. LNO)

Material	D^* (cm^2/s)	k^* (cm/s)
LNO ³	1.0×10^{-6}	1.5×10^{-8}
Pr_6O_{11} ⁵	3.4×10^{-8}	5.4×10^{-7}

➤ **Pr_6O_{11} could behave similar to LSM**
(detailed study of charge transfer mechanisms required)

Preparation of a triple layer composite Pr_6O_{11} -GDC electrode

ESD -“infiltration” of porous GDC - conditions

$$d_{size} \propto \left(\frac{\rho \varepsilon_0 Q^3}{\gamma \sigma} \right)^{1/6}$$

- **Smallest particles possible**

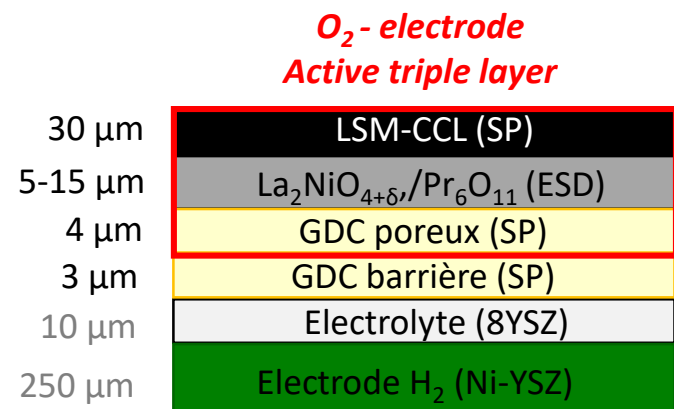
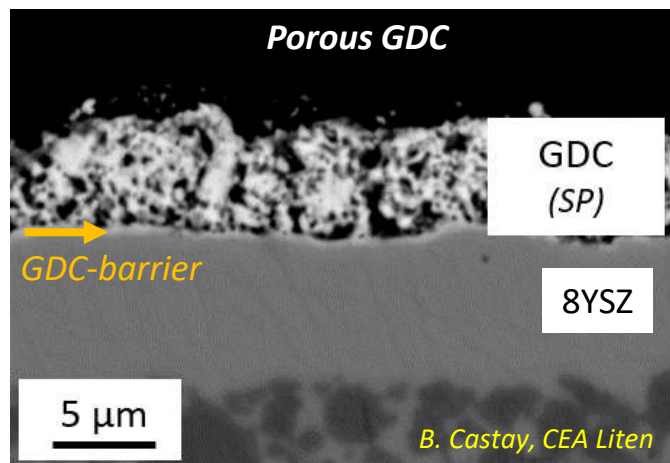
Solvent = $\text{EtOH} : \text{H}_2\text{O}$ (1:2, vol.)

$T = 350^\circ\text{C}$

$d = 50\text{ mm}$

$Q = 1.0\text{ mL/h}$

Sample preparation



Thank you for your attention!

Acknowledgements



R. Sharma (Ph.D, 2016)



N. Khamidy (Ph.D, 2020)

LABEX CEMAM



L. Yefsah (Ph.D student)

ANR ECOREVE



E. Djurado
C. Steil
L. Dessemond
F. Fournet-Fayard



J. Laurencin
B. Castay



Infiltration using precursors

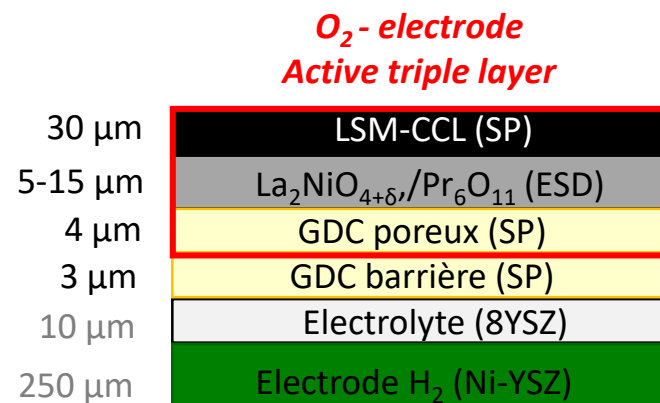
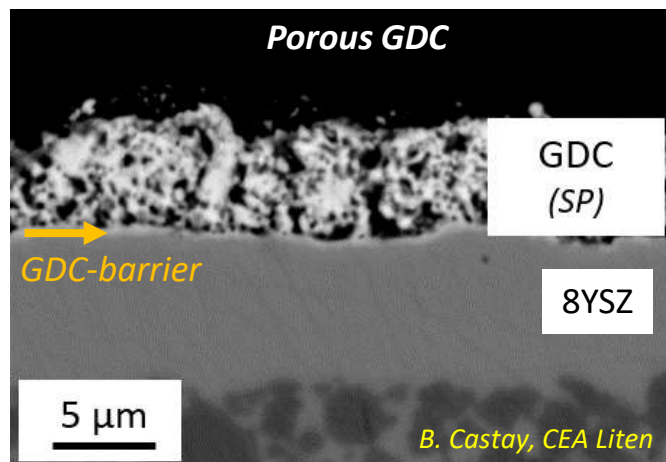
- R_{pol} (650 °C, air) = 0.16 Ω cm²
NV Lyskov, Russ. J. Electrochim., 57 (2021), 1070
- R_{pol} (600 °C, air) = 0.074 Ω cm²
M Khoshkalam, J. Electrochim. Soc., 167 (2020), 024505
- R_{pol} (600 °C, air) = 0.028 Ω cm²
C Nicollet, Int. J. Hydrg. Energy, 41 (2016), 15538
- 1.56 W cm⁻² at 700 °C (PrOx in AFL)
E Dogdibegovic, J. Power Sources., 410 (2019), 91
- - 1.5 A cm⁻² at 1.4 V (50 vol.% steam on H₂ side, 700 °C)
R Wang, Energy Technol., 7 (2019), 1801154

ESD -“infiltration” of porous GDC - conditions

$$d_{\text{size}} \propto \left(\frac{\rho \epsilon_0 Q^3}{\gamma \sigma} \right)^{1/6}$$

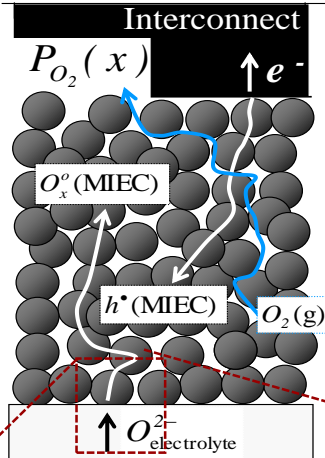
- **Smallest particles possible**
Solvent = EtOH : H₂O (1:2, vol.)
 $T = 350$ °C
 $d = 50$ mm
 $Q = 1.0$ mL/h

Sample preparation



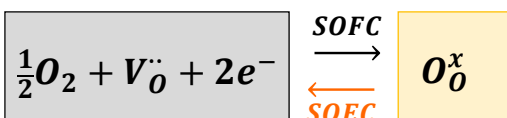
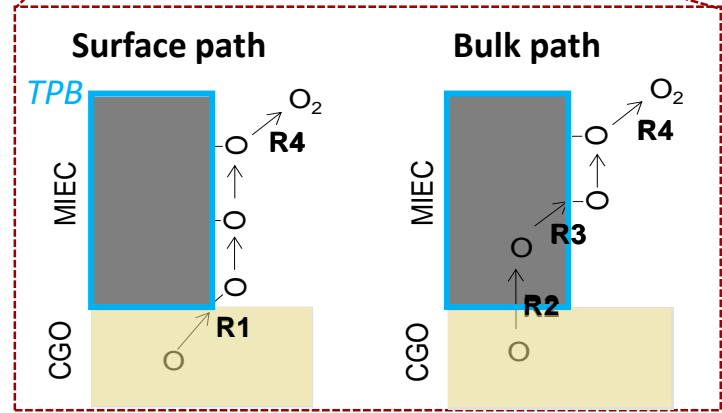
Perspectives: composite oxygen electrodes

SOEC mode (for LNO)

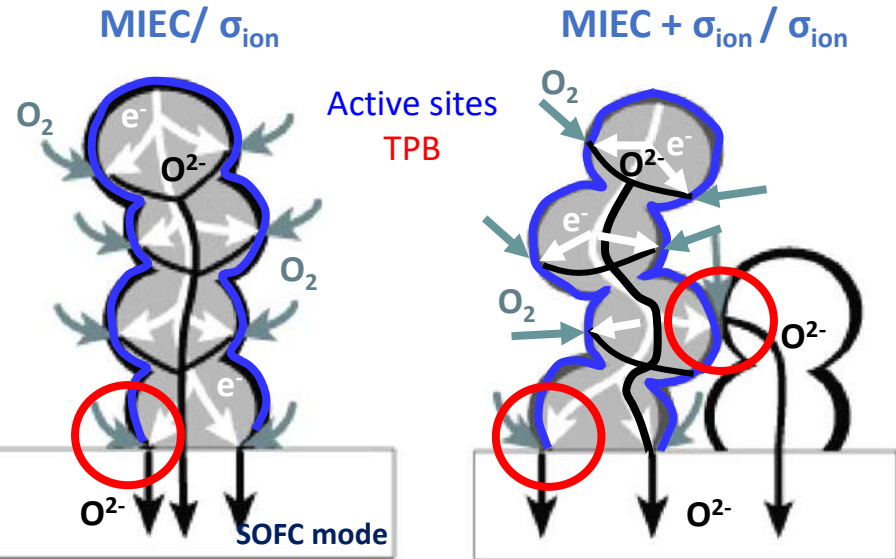


- R1: Direct oxidation at TPB
- R2: Ionic transfer (electrolyte to electrode)
- R3: Interstitial diffusion + excorporation + formation of adatoms
- R4: Association + desorption

G Sdanghi, J. Electrochem. Soc., 169 (2022), 034518
L Yefsah, (2023) PhD Thesis, UGA



- ✓ SOEC: filling of interstitials, parallel surface + bulk path, stable
- ✗ SOFC: depletion of interstitials (bulk path limiting)
 1. Performance
 2. Physical delamination (e.g. LNO)



Adapted from: S REY-MERMET, (2008) PhD Thesis, EPFL

Dominant surface path
→ increase number of TPB

Increase interface with ionic conductor

Material	D^* (cm ² /s)	k^* (cm/s)
LNO ³	1.0×10^{-6}	1.5×10^{-8}
PNO ⁴	5.0×10^{-7}	2.5×10^{-8}
Pr ₆ O ₁₁ ⁵	3.4×10^{-8}	5.4×10^{-7}

¹ De Souza, Solid State Ion., 106 (1998), 175; ² Audinot, (1998) Université de Bordeaux; ³ Skinner, Solid State Ion., 135 (2000), 70; ⁴ Solid State Ion., 176 (2005), 2717; ⁵ Nicollet, Int. J. Hydrog. Energy, 41 (2016), 1000.